

Frustrated Spin Systems

Frédéric Mila

Institute of Theoretical Physics

Ecole Polytechnique Fédérale de Lausanne

1015 Lausanne, Switzerland

Contents

1	Introduction	2
2	Competing interactions and degeneracy	3
2.1	Ising	3
2.2	Heisenberg	6
3	Classical ground state correlations	8
3.1	Algebraic correlations	8
3.2	Dipolar correlations	10
4	Order by disorder	12
4.1	Quantum fluctuations	12
4.2	Thermal fluctuations	14
5	Alternatives to magnetic long-range order in Heisenberg models	14
5.1	Spin gap	15
5.2	Resonating Valence Bond spin liquids	17
5.3	Algebraic spin liquids	21
5.4	Chiral spin liquids	23
5.5	Nematic order	24
6	Conclusion	27

1 Introduction

In the field of magnetism, the word frustration has first been introduced in the context of spin glasses to describe the impossibility to satisfy simultaneously all exchange processes. In this lecture, we are primarily interested in disorder-free systems that can be described by a periodic Hamiltonian. In that case, frustration is more precisely described as *geometrical frustration*, a concept that has received the following general definition: one speaks of *geometrical frustration* when a local condition is unable to lead to a simple pattern for an extended system [1]. Typical examples are paving problems, where some figures such as triangles in two dimensions lead to regular, packed pavings while others such as pentagons are unable to lead to a compact, periodic structure.

In this lecture, we will be dealing mostly with two models of magnetism: the *Ising* model

$$H = \sum_{(i,j)} J_{ij} S_i S_j, \quad S_i, S_j = \pm 1 \text{ or } \uparrow, \downarrow \quad (1)$$

and the *Heisenberg* model

$$H = \sum_{(i,j)} J_{ij} \vec{S}_i \cdot \vec{S}_j \quad (2)$$

where the spins \vec{S}_i are unit vectors in the *classical* case, and components of a quantum spin in the *quantum* case: $[S_i^\alpha, S_i^\beta] = i\epsilon^{\alpha\beta\gamma} S_i^\gamma$, and $\vec{S}_i^2 = S(S+1)$. In both cases, i and j are sites of a periodic lattice, and J_{ij} is assumed to depend only on their relative position.

Frustration can only occur if at least some exchange paths are antiferromagnetic, i.e. if some of the exchange integrals J_{ij} are positive since, if all exchange paths are ferromagnetic with negative exchange integrals, the configuration with all spins parallel is clearly the ground state. However, even when all bonds are antiferromagnetic, geometrical frustration is not necessarily realized. Indeed, for bipartite lattices such as the square lattice, that can be divided into two sublattices such that each spin of one sublattice is only coupled to spins of the other sublattice, the energy of the Ising model or of the classical Heisenberg model is simply minimized by the Néel configuration in which the spins of one sublattice are parallel to each other and antiparallel to all spins of the other sublattice.

A necessary condition to satisfy the general condition of geometrical frustration with only antiferromagnetic exchange interactions is to have loops of odd length. This is however *not* sufficient. Indeed, as we shall see, it is often possible to minimize the energy of the classical antiferromagnetic Heisenberg model with a simple helical arrangement of spins, and if this defines a unique ground state, as in the case of the triangular lattice with nearest-neighbor interactions, the system is strictly speaking not geometrically frustrated: Geometrical frustration occurs when there is not a unique way to minimize the energy, but when there are other ways with less simple (often non periodic) structures to reach the ground state energy.

The objective of this lecture is to review the physical consequences of this degeneracy from a theoretical perspective. For Ising spins, degeneracy can lead to all types of zero temperature behaviors: long-range order, algebraic order, dipolar correlations or complete disorder. For

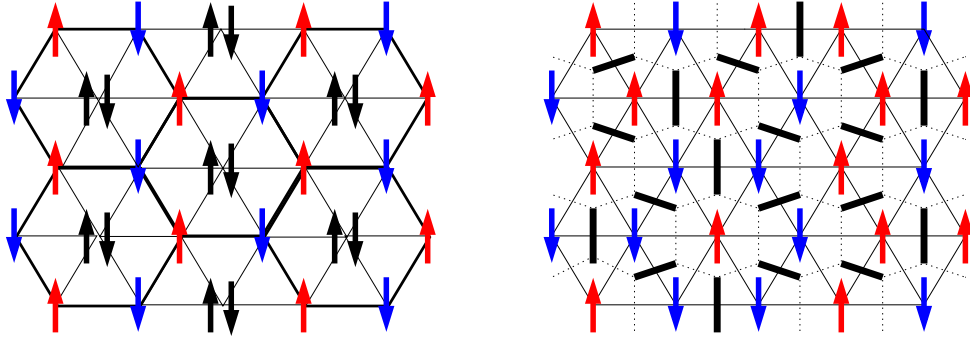


Fig. 1: *Left panel: Example of degenerate ground states of the antiferromagnetic Ising model on the triangular lattice. Once spins have been arranged antiferromagnetically on a honeycomb sublattice (thick solid line), the spins in the center of the hexagons can point up or down. Right panel: Mapping between a ground state of the Ising model on the triangular lattice and a dimer covering on the dual honeycomb lattice. The bonds of the triangular lattice with parallel spins are crossed by a dimer.*

Heisenberg models, fluctuations (thermal or quantum) play a major role. They can order the system by picking one ordered state out of the ground state manifold, but they can also destroy any kind of magnetic long-range order. This opens the way to new types of ground states such as spin nematics (where the order parameter is not the local spin but a more complicated object), valence-bond crystals (completely non-magnetic states with a broken translational symmetry), or quantum spin liquids where both the rotational $SU(2)$ symmetry in spin space and the translation symmetry in real space are preserved.

2 Competing interactions and degeneracy

2.1 Ising

For the Ising model, competing interactions generically lead to an infinite degeneracy. As a first hint, let us consider the antiferromagnetic Ising model on the triangular lattice. On a triangle, the best one can do it to satisfy two bonds out of three, and any configuration with two up spins and one down spin or two down spins and one up spin on each triangle minimizes the energy. A simple way to satisfy this condition is to look at the triangular lattice as a centered honeycomb lattice. Then, if the honeycomb lattice is in a Néel state, the condition will be automatically satisfied regardless of the orientation of the spins inside the hexagons (see left panel of Fig. 1). So the ground state degeneracy is at least equal to $2^{N/3}$, where N is the number of sites, and there is a residual entropy per site bounded from below by $(1/3) \ln 2 \simeq 0.2310$. In fact, the residual entropy is much larger, as first shown by Wannier [2], who derived the exact result $S/N = 0.3230\dots$

A useful way to derive this result for the purpose of this lecture is to map the problem onto that of the dimer coverings on the dual honeycomb lattice by putting a dimer across each unsatisfied bond of a ground state of the Ising model [3] (see right panel of Fig. 1). Up to a factor 2 asso-

ciated to overturning all spins, there is a one to one correspondence. The problem of counting the dimer coverings on a planar graph has been addressed in the early sixties [4, 5], and the following theorem has been proven:

Theorem: If one can attach to each adjacent pair of sites an arrow such that, around each loop with an even number of sites, the number of arrows in each direction is odd, the total number of dimer coverings can be expressed as the determinant of a periodic, skew-symmetric matrix.

Proof: The number of dimer coverings is clearly given by

$$Z = \frac{1}{\left(\frac{N}{2}\right)! 2^{N/2}} \sum_P b(p_1, p_2) b(p_3, p_4) \dots b(p_{N-1}, p_N)$$

where the sum over $P = \{p_1, \dots, p_N\}$ runs over the permutations of $1, \dots, N$, and

$$b(i, j) = \begin{cases} 1 & \text{if } i, j \text{ adjacent,} \\ 0 & \text{otherwise.} \end{cases}$$

Now, define the skew-symmetric Kasteleyn matrix $a(i, j)$ by:

$$a(i, j) = \begin{cases} 1 & \text{if } i, j \text{ adjacent and } i \rightarrow j \\ -1 & \text{if } i, j \text{ adjacent and } i \leftarrow j \\ 0 & \text{otherwise.} \end{cases}$$

where $i \rightarrow j$ means that the arrow goes from i to j . Then,

$$Z = \left| \frac{1}{\left(\frac{N}{2}\right)! 2^{N/2}} \sum_P \varepsilon(P) a(p_1, p_2) \dots a(p_{N-1}, p_N) \right|$$

where $\varepsilon(P)$ is the signature of the permutation. Indeed, this will be clearly true if, for all permutations, i.e. for all dimer coverings, the sign of $\varepsilon(P) a(p_1, p_2) \dots a(p_{N-1}, p_N)$ is the same. Now, consider 2 dimer coverings C and C' . To go from one to the other, one just has to shift sites around loops of even length. For the sites of a given loop, the product of the matrix elements of C and C' will be negative because, thanks to the hypothesis of the theorem, the number of arrows in each direction is odd. Besides, the signature of the permutation is negative because the number of sites is even. So, each loop contributes a factor with the same sign for C and C' , and the terms in the sum corresponding to C and C' have the same sign, which implies that the terms in the sum have the same sign for all dimer coverings.

Now, the sum over P is the pfaffian of the skew-symmetric matrix $a(i, j)$, and its square is equal to the determinant of a . So finally,

$$Z = \sqrt{\det a}$$

The determinant is the product of the eigenvalues of a , which, on a periodic lattice, can be easily calculated using Bloch theorem. In the case of the honeycomb lattice, this leads to:

$$\frac{1}{N_{hc}} \ln Z = \frac{1}{4} \int_0^1 dx \int_0^1 dy \ln |3 + 2 \cos(2\pi y) - 2 \cos(2\pi(x + y)) - 2 \cos(2\pi x)| \simeq 0.1615$$

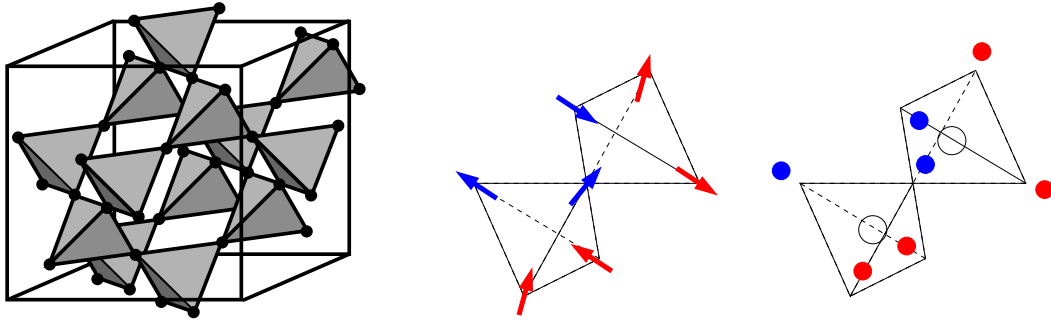


Fig. 2: Left panel: sketch of the pyrochlore lattice. Middle panel: example of a 2-in 2-out structure stabilized in spin ice. Right panel: same configuration as that of the middle panel, but for water ice, the blue and red dots standing for H atoms. Each oxygen atom (empty circle) forms an H_2O molecule with the two hydrogen atoms close to it.

Since the number of sites of the honeycomb lattice $N_{hc} = N/2$, the entropy per site for the Ising model is given by $S/N = 0.3230 \dots$, in agreement with Wannier's result [2].

When the mapping on an exactly soluble dimer covering problem is not possible, one can always resort to a numerical enumeration of all configurations to estimate the residual entropy. However, it is often possible to get a good estimate with the help of a simple argument developed by Pauling in the context of ice [6]. Let us consider the case of $Dy_2Ti_2O_7$ and $Ho_2Ti_2O_7$ [7]. In these systems, known as spin ice systems, classical spins sit on a pyrochlore lattice (see left panel of Fig. 2). They have to point along the direction joining the site where they sit to the centers of the neighboring tetrahedra, and the interaction is ferromagnetic. Then, on a tetrahedron, the energy is minimized for configurations with two spins in and two spins out (see middle panel of Fig. 2). This model can be mapped onto the problem of water ice, in which oxygen atoms sit at the center of the tetrahedra of a pyrochlore lattice, and the hydrogen atoms sit in principle on the pyrochlore lattice, but on each tetrahedron two of them get closer to the oxygen to form a water molecule H_2O (see right panel of Fig. 2). Remarkably, it can also be mapped onto the antiferromagnetic Ising model on the pyrochlore lattice, with two spins up and two spins down on each tetrahedron.

To estimate the entropy, Pauling noted that, on a given tetrahedron, there are in total $2^4 = 16$ configurations, but only 6 of them satisfy the constraint. So, to estimate the number of configurations for a system of N sites, he suggested to multiply the total number of configurations, 2^N , by 6/16 per tetrahedron. Since the number of tetrahedra is $N/2$, this gives:

$$Z \approx 2^N \left(\frac{6}{16} \right)^{\frac{N}{2}} = \left(\frac{3}{2} \right)^{N/2}$$

leading to

$$\frac{S}{N} = \frac{1}{2} \ln \left(\frac{3}{2} \right) = 0.2027$$

This estimate compares remarkably well with the 'exact' numerical result $S/N = 0.20501\dots$ [8]. Even more remarkably, this value has been measured experimentally in $Dy_2Ti_2O_7$ [9].

Indeed, the entropy per site at high temperature is equal to $\ln 2$, and if the ground state is degenerate, the residual entropy can be determined as:

$$S/N = \ln 2 - \int_{0^+}^{+\infty} \frac{C(T)dT}{T} \quad (3)$$

where $C(T)$ is the specific heat.

2.2 Heisenberg

For the Heisenberg model, frustration is often used, by analogy with the Ising case, as a synonym of competing interactions, but the effects to be discussed below occur when the competition is so severe that, for classical spins, the ground state is infinitely generate. That this is not always the case is clear from the following theorem [10]:

Theorem: On a Bravais lattice (i.e. a lattice with one site per unit cell), the classical energy is minimized by a helical structure $\vec{S}_{\vec{R}_i} = (\cos(\vec{k} \cdot \vec{R}_i), \sin(\vec{k} \cdot \vec{R}_i), 0)$, where \vec{k} is a minimum of the Fourier transform of the coupling constant $J(\vec{k}) = \sum_{\vec{R}_j} J_{\vec{R}_i \vec{R}_j} \exp[i\vec{k} \cdot (\vec{R}_j - \vec{R}_i)]$.

Proof: This theorem is easily proven by first replacing the local constraint $||\vec{S}_i||^2 = 1$ by a global one $\sum_i ||\vec{S}_i||^2 = N$, and by looking for a specific solution of the global constraint that satisfies the local constraint.

In fact, even on non-Bravais lattices, it is often possible to minimize the energy with some kind of helical state. However, the fact that the energy can be minimized by a regular structure does not imply that this is the only one. Let us demonstrate this in a few representative cases.

2.2.1 $J_1 - J_2$ model on the square lattice

For the Heisenberg model on the square lattice with nearest-neighbour coupling J_1 and next-nearest neighbour coupling J_2 (see left panel of Fig. 3), the Fourier transform of the coupling constant is given by:

$$J(\vec{k}) = 2J_1(\cos k_x + \cos k_y) + 4J_2 \cos k_x \cos k_y \quad (4)$$

As long as $J_1 > 2J_2 > 0$, the minimum is reached for $\vec{k} = (\pi, \pi)$, and the ground state has Néel order. However, when $J_2 > J_1/2 > 0$, $J(\vec{k})$ is minimized by two wave-vectors: $\vec{k} = (0, \pi)$ and $\vec{k} = (\pi, 0)$. So the minimum energy is reached for two helical states. Quite remarkably, the energy per site is given by $E/N = -2J_2$ and does not depend on J_1 . This is a consequence of the fact that in these states the two sublattices are Néel ordered, so that J_1 couples any spin to two pairs of spins pointing in opposite directions and drops from the energy. But this remains true regardless of the relative angle θ between the spins of each sublattice, so that the ground state manifold consists of all states with Néel ordered sublattices (see left panel of Fig. 3). The ground state is thus infinitely degenerate, and the degeneracy is controlled by a continuous parameter, the angle θ between the sublattices.

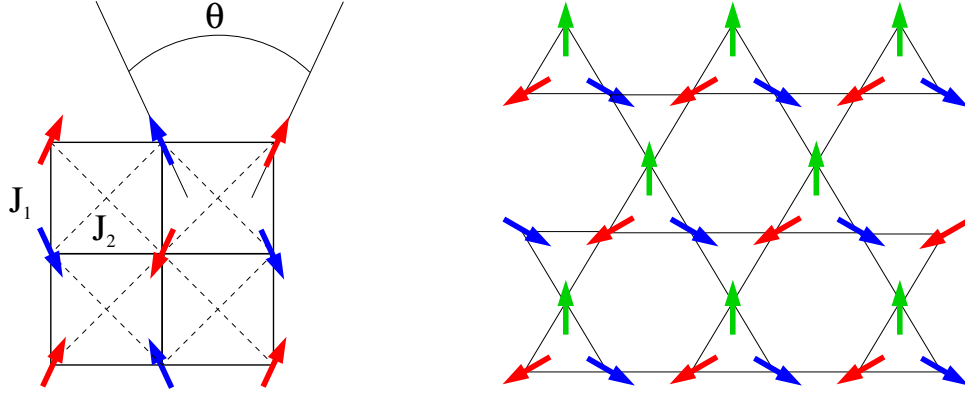


Fig. 3: Left panel: sketch of the ground state of the $J_1 - J_2$ model on the square lattice for $J_2 > J_1/2$. Each sublattice has Néel order. The ground state energy is independent of the angle θ between the spins on the two sublattices. Right panel: $\vec{q} = \vec{0}$ ground state of the classical Heisenberg model on the kagome lattice. New, non-coplanar ground states can be generated by rotating the spins along any line (e.g. the red and blue spins of a horizontal line) around the common direction of the spins to which they are coupled (e.g. the vertical direction of the green spins)

2.2.2 Kagome lattice

For three spins, the classical Heisenberg model is proportional to

$$\vec{S}_1 \cdot \vec{S}_2 + \vec{S}_2 \cdot \vec{S}_3 + \vec{S}_3 \cdot \vec{S}_1 = \frac{1}{2}(\vec{S}_1 + \vec{S}_2 + \vec{S}_3)^2 - \frac{3}{2}$$

This expression is minimized as soon as $\vec{S}_1 + \vec{S}_2 + \vec{S}_3 = \vec{0}$. So, for antiferromagnets built out of triangles, a sufficient condition to minimize the energy is to find a configuration for which this constraint is satisfied on all triangles. For the triangular lattice, this condition leads, up to a global rotation of the spins, to a unique three-sublattice helical state. However, for the kagome lattice, which consists of corner sharing triangles, this can be satisfied in an infinite number of ways. For coplanar configurations, once the direction of one spin has been chosen, the problem is equivalent to the antiferromagnetic 3-state Potts model, which is known to have an infinitely degenerate ground state with an extensive residual entropy [11]. This leads to an infinite, discrete degeneracy. But the situation is far richer. Consider for instance the ground state in which all up triangles have the same pattern (see right panel of Fig. 3). Non-coplanar ground states can be constructed by rotating the spins along any line around the common direction of the spins adjacent to it. This can be done independently on all lines parallel to a given direction. More generally, starting from any ground state, the spins inside a cluster surrounded by identical spins can be freely rotated. So the degeneracy is controlled by an infinite number of continuous variables.

2.2.3 Pyrochlore

The situation is similar for the three-dimensional pyrochlore lattice. All the states that satisfy the constraint $\vec{S}_1 + \vec{S}_2 + \vec{S}_3 + \vec{S}_4 = \vec{0}$ on each tetrahedron are ground states. This constraint can be satisfied in many ways, and new ground states can often be generated by rotations of subsets of spins.

3 Classical ground state correlations

When the classical ground state of a model is infinitely degenerate, zero-temperature correlations are naturally defined as the average over all ground states. Naively, one could imagine that averaging over an infinite number of different states will generically lead to effective disorder, but quite remarkably this is not the case, and most systems that have an infinite but discrete ground state degeneracy turn out to exhibit algebraic correlations, sometimes of dipolar type, although some are completely disordered (e.g. the antiferromagnetic model on the kagome lattice [12]), and some long-range ordered (e.g. the 3-states Potts model on the dice lattice [13] or the bilinear-biquadratic Heisenberg model on the triangular lattice [14]).

3.1 Algebraic correlations

A well known example of algebraic correlations is provided by the AF Ising model on the triangular lattice. The original proof by Stephenson [15] that the correlations decay as $1/r^{1/2}$ is too involved to be reproduced here, but this result can be made plausible thanks to the mapping onto the dimer problem on the honeycomb lattice. Indeed, the Pfaffian that enters the calculation of the number of dimer coverings can be reformulated in terms of an integral over Grassman variables, and the Green function between Grassman variables at sites i and j is the matrix element $(a^{-1})_{ij}$, where a is the Kasteleyn matrix. Now, in Fourier space, the spectrum of the Kasteleyn matrix has Dirac point at zero eigenvalue for the honeycomb lattice. This implies that the Green's function decays algebraically at long distance. Using Wick theorem, this in turn implies that more complicated correlations such as dimer-dimer correlations in the dimer covering problem or spin-spin correlations in the Ising model should also decay algebraically. Intuitively, the presence of algebraic correlations suggests that the system is almost ordered, and that configurations that are not too far from a specific one dominate the sum. A plausible condition for this specific configuration is to be maximally flippable, i.e. connected by individual spin flips to a maximal number of allowed configurations. To implement this idea, it has been suggested to map these models onto height models [16, 17], the maximally flippable state corresponding to a flat surface. Such models represent the fluctuations of the surface of a solid by assigning to each point a height. They describe the roughening transition of a solid between a flat surface, where the height difference is bounded from above, and a rough surface, where height differences diverge [18].

For the triangular Ising antiferromagnet, the mapping onto height variables proceeds in two steps. First of all, microscopic height variables $z(\vec{r})$ are defined on the vertices of the original

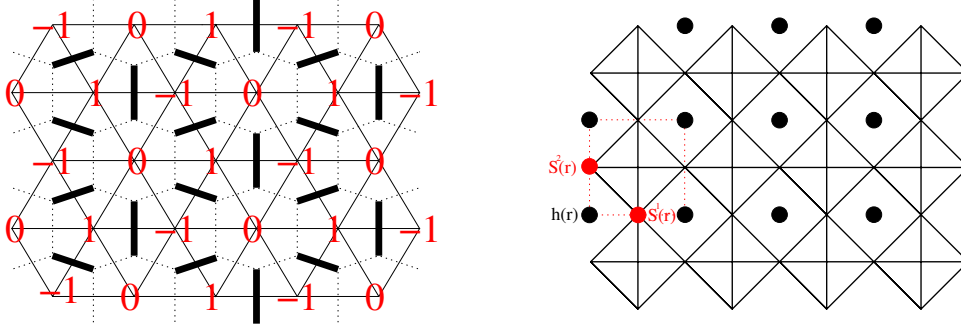


Fig. 4: Left panel: height mapping of the Ising model on the triangular lattice. The configuration represented here is the flat one. It corresponds to the maximally flippable configuration in terms of Ising spins (not shown). Right panel: sketch of the mapping of the Ising model on the checkerboard lattice on a height model. The dotted red line is the unit cell.

triangle lattice (see left panel of Fig. 4). To each ground state of the Ising model, one first associates a dimer covering of the dual honeycomb lattice. Then, after choosing the height of one site, one associates to each dimer covering a height configuration following the prescription that, when going clockwise around an up triangle, the height difference between neighboring sites is equal to 2 if one crosses a dimer and -1 if one does not cross a dimer. With this prescription, the height differences around all triangles (up and down) is zero, and the assignment is consistent.

Next, one defines a smooth height field on the dual lattice $h(\vec{x})$ by coarse-graining the field $z(\vec{r})$, i.e. by averaging it on each triangular plaquette:

$$h(\vec{x}) = [z(\vec{r}_1) + z(\vec{r}_2) + z(\vec{r}_3)]/3$$

where \vec{r}_1 , \vec{r}_2 and \vec{r}_3 are the sites of a triangle, and $\vec{x} = (\vec{r}_1 + \vec{r}_2 + \vec{r}_3)/3$ is a site of the dual lattice.

The idea is now to describe the ground state manifold as fluctuations around the flat surface, where the height variable is almost the same everywhere. With the prescription above, this correspond to the configuration shown in the left panel of Fig. 4, in which $h(\vec{x}) = 0$ on all triangles. So it is natural to assume that this height configuration has a maximal weight, and that other height configurations will be penalized. The simplest assumption is a gaussian weight. Going to a continuous height variable, one assume a free energy of the form:

$$F(\{h(\vec{x})\}) = \int d\vec{x} \frac{K}{2} |\vec{\nabla} h(\vec{x})|^2 = \sum_{\vec{q}} \frac{K}{2} q^2 |h(\vec{q})|^2$$

For a mode $h(\vec{q})$, the mean value of $h(\vec{q})^2$ is given by:

$$\langle |h(\vec{q})|^2 \rangle = \frac{\int dh h^2 \exp(-\frac{K}{2} q^2 h^2)}{\int dh \exp(-\frac{K}{2} q^2 h^2)} = \frac{1}{K q^2}$$

which implies that

$$C(\vec{r}) \equiv \frac{1}{2} \langle |h(\vec{r}) - h(\vec{0})|^2 \rangle = \int d\vec{q} (1 - e^{i\vec{q} \cdot \vec{r}}) \frac{1}{K q^2} \propto \frac{1}{2\pi K} \ln \frac{\pi r}{\alpha}, \quad r \rightarrow +\infty$$

To extract the correlations of the Ising model, one must relate the spin variables $\sigma_{\vec{r}_i}$ to the height variables. This relation is not simple, but it is enough to realize that the spin variables have to be periodic functions of the height variables of period 6. Indeed, turning the spins around a triangle twice leads to the same configuration, while the height has changed by 6. So any local operator of the spin $O(\vec{r})$ can be expanded as

$$O(\vec{r}) = \sum_{G \neq 0} O_G e^{iGh(\vec{r})}$$

with $G = 2\pi n/6$, n integer. Using the identity

$$\langle e^{-iG[h(\vec{r})-h(\vec{0})]} \rangle = e^{-\frac{1}{2}G^2 \langle |h(\vec{r})-h(\vec{0})|^2 \rangle}$$

it is clear that the long-range correlations are dominated by the smallest value of G . So one can assume $\sigma(\vec{r}) \propto e^{i\frac{2\pi}{6}h(\vec{r})}$ to calculate the long range correlations, which leads to:

$$\langle \sigma(\vec{r})\sigma(\vec{0}) \rangle \propto \left(\frac{\pi r}{a}\right)^{-\left(\frac{2\pi}{6}\right)^2 \frac{1}{2\pi K}} = \left(\frac{\pi r}{a}\right)^{-\frac{2\pi}{36K}}$$

Comparing this result with the exact result that the correlations decay as $1/r^{1/2}$, one gets $K = \pi/9$. This shows that the system is in the rough phase where $\langle |h(\vec{r}) - h(\vec{0})|^2 \rangle$ diverges logarithmically since this phase is stable as long as $K < \pi/2$.

3.2 Dipolar correlations

The checkerboard lattice (see right panel of Fig. 4) is another example of a frustrated lattice on which the Ising model is infinitely degenerate, the rule in the ground state being that $\sum_{\square} S_i = 0$ for all plaquettes with diagonal bonds. This is not a planar graph (bonds are crossing), and a mapping onto a dimer model is not possible. So the form of the long range correlations cannot be guessed from the spectrum of a Kasteleyn matrix. The height mapping is in that case very useful, and it brings an unexpected new feature of the correlations [17].

The mapping works as follows (see Fig. 4, right panel): The height variables are numbers defined in the squares without diagonal bonds and related to the spins by

$$\begin{cases} S^1(\vec{r}) = (-1)^{x+y} \Delta_x h \\ S^2(\vec{r}) = (-1)^{x+y} \Delta_y h \end{cases}$$

where $S^1(\vec{r})$ and $S^2(\vec{r})$ refer to the two spins in the unit cell.

In that case, the spin is related to the height field by:

$$S^i(\vec{r}) = (-1)^{x+y} \partial_{x_i} h + e^{i\pi h} + \dots$$

The dominant contribution to the correlations comes from the first term:

$$\langle S^i(\vec{r}) S^j(\vec{0}) \rangle = (-1)^{x+y} \partial_{x_i} \partial_{x_j} C(\vec{r}) \propto \frac{(-1)^{x+y}}{2\pi K} \partial_{x_i} \partial_{x_j} \ln \left(\frac{\pi r}{\alpha} \right)$$

which finally leads to

$$\left\langle S^i(\vec{r}) S^j(\vec{0}) \right\rangle = \frac{(-1)^{x+y}}{2\pi K} \frac{r^2 \delta_{ij} - 2x_i x_j}{r^4} \quad (5)$$

These correlations have a dipolar form.¹

The situation is very similar for the pyrochlore lattice with antiferromagnetic couplings [19], but the effective model is a lattice gauge theory. In the ground state, the rule for each tetrahedron is that

$$\sum_{\boxtimes} S_i = 0$$

Consider the dual lattice of the pyrochlore lattice. This is the diamond lattice, a bipartite lattice. Divide it into two sublattices A and B and on each bond κ define a unit vector \hat{e}_κ from A to B . Next, define a field on the site of the original lattice, hence on the bond of the diamond lattice, by:

$$\vec{B}_\kappa = S_\kappa \hat{e}_\kappa$$

The lattice version of the integral of the divergence around a site \vec{x} of the diamond lattice is given by

$$\sum_{\kappa(\vec{x})} \vec{B}_\kappa \cdot \hat{e}_\kappa = \sum_{\kappa(\vec{x})} S_\kappa = 0$$

because of the local rule in the ground state manifold of the AF Ising model on the pyrochlore lattice.

So, one can look in the continuum for a field with zero divergence. Upon coarse graining, the configurations with small coarse grained field \vec{B} are favoured. Indeed, to go from one ground state to the other one must flip the spins along a loop of alternating spins to fulfill the constraint $\sum_{\boxtimes} S_i = 0$. Along such loops, the sum of the field $\vec{B}_\kappa = \vec{0}$. This implies that configurations with a very small \vec{B} will have small loops of \vec{B}_κ and will be very flippable.

So, one can postulate a weight

$$S(\vec{B}(\vec{x})) = \exp \left[-\frac{K}{2} \int d^3\vec{r} \vec{B}(\vec{r})^2 \right] \quad (6)$$

Since $\text{div} \vec{B} = 0$, one can choose a vector potential \vec{A} such that $\vec{B} = \vec{\nabla} \times \vec{A}$. With the gauge $\text{div} \vec{A} = 0$, its correlations are given by:

$$\langle |A(\vec{q})|^2 \rangle = \frac{1}{Kq^2}$$

or in real space by

$$\left\langle A_i(\vec{r}) A_j(\vec{0}) \right\rangle = \frac{\delta_{ij}}{4\pi K r}$$

¹The mapping onto a height model leads generically to algebraic, and often dipolar, correlations. What makes the height mapping possible? The mapping is possible if a height configuration leads to a single spin configuration, and a spin configuration to a single height configuration up to a global shift. Since the height is single valued one has to go back to the same height around basic loops. For this to occur, elementary loops for the height should be constrained by a local condition in the ground state manifold. This is the case for the triangular lattice ($\sum_i \sigma_i = \pm 1$, never 3 or -3), and for the checkerboard lattice ($\sum_{\boxtimes} S_i = 0$).

This leads to the correlations of the \vec{B} field

$$\langle B_i(\vec{r}) B_j(\vec{0}) \rangle = \frac{1}{4\pi K} \frac{3x_i x_j - \delta_{ij} r^2}{r^5}$$

and finally to the spin-spin correlations

$$\langle S_\alpha(\vec{r}) S_\beta(\vec{0}) \rangle = \frac{1}{4\pi K} \frac{3(\hat{e}_\alpha \cdot \vec{r})(\hat{e}_\beta \cdot \vec{r}) - (\hat{e}_\alpha \cdot \hat{e}_\beta) r^2}{r^5} \quad (7)$$

where α and β keep track of the position of the spin in the unit cell.

The dipolar form of the correlations leads to a very specific signature, namely the presence of pinch points in diffuse scattering [20, 21].

4 Order by disorder

If the ground state of a classical Heisenberg model has no long-range magnetic order because of geometrical frustration, it does not necessarily imply that this remains true at $T > 0$, or for the quantum version of the model [22–24]. Indeed, the spectrum of fluctuations usually depends on the ground state, and this can lead to a selection mechanism known as 'order by disorder' that can lead to long-range magnetic order.

4.1 Quantum fluctuations

Let us start by discussing the effect of quantum fluctuations. When spin are quantum operators, the fluctuations around a given ground state can be described at the harmonic level with the help of the Holstein-Primakoff transformation:

$$\begin{cases} S_i^{z_i} = S - a_i^\dagger a_i \\ S_i^+ = \sqrt{2S - a_i^\dagger a_i} a_i \\ S_i^- = a_i^\dagger \sqrt{2S - a_i^\dagger a_i} \end{cases} \quad (8)$$

where the quantization axis z_i is in the direction of the spin at site i in the ground state under consideration. Keeping only terms of order S^2 and S leads to a quadratic Hamiltonian. If the environment of all sites is the same up to a rotation (a condition which is often met even if the ground state is not periodic, as for instance in helical states on a Bravais lattice), the Hamiltonian takes the general form in Fourier space:

$$H = E_{\text{classical}} + \sum_{\vec{k}} \left[B_{\vec{k}} a_{\vec{k}}^\dagger a_{\vec{k}} + \frac{1}{2} A_{\vec{k}} \left(a_{\vec{k}}^\dagger a_{-\vec{k}}^\dagger + a_{\vec{k}} a_{-\vec{k}} \right) \right]$$

where $E_{\text{classical}}$ is proportional to S^2 and $A_{\vec{k}}$ and $B_{\vec{k}}$ are coefficients proportional to S that depend on the exchange integrals and on the ground state. This Hamiltonian can be put in diagonal form

$$\mathcal{H} = E_0 + \sum_{\vec{k}} \omega_{\vec{k}} \left(\alpha_{\vec{k}}^\dagger \alpha_{\vec{k}} + \frac{1}{2} \right)$$

where the operators $\alpha_{\vec{k}}^\dagger$ and $\alpha_{\vec{k}}$ are related to the Holstein-Primakoff operators by a Bogoliubov transformation:

$$\alpha_{\vec{k}} = u_{\vec{k}} a_{\vec{k}} + v_{\vec{k}} a_{-\vec{k}}^\dagger$$

with

$$\omega_{\vec{k}} = \sqrt{B_{\vec{k}}^2 - A_{\vec{k}}^2}, \quad u_{\vec{k}} = \sqrt{\frac{B_{\vec{k}} + \omega_{\vec{k}}}{2\omega_{\vec{k}}}}, \quad v_{\vec{k}} = \text{sign}(A_{\vec{k}}) \sqrt{\frac{B_{\vec{k}} - \omega_{\vec{k}}}{2\omega_{\vec{k}}}}$$

In Eq.(4.1), the energy E_0 is the sum of the classical energy, which is independent of the ground state, and of a quantum correction also independent of the ground state. For antiferromagnetic bonds, its expression is the same as that of the classical energy up to the replacement $S^2 \rightarrow S(S+1)$.

Then, the energy of the quantum state obtained by 'dressing' a classical state with quantum fluctuations includes a zero point contribution and is given by:

$$E(\theta) = E_0 + \frac{1}{2} \sum_{\vec{k}} \omega_{\vec{k}}(\theta) \quad (9)$$

In that expression, θ stands for a parameter (or a set of parameters) that runs over the degenerate ground state manifold, and we have made it explicit that the right hand side depends on θ through $\omega_{\vec{k}}$, which is the case because the coefficients $A_{\vec{k}}$ and $B_{\vec{k}}$ depend on the ground state. If the minimization of this energy with respect to θ selects a value of θ for which the classical ground state has long-range order, then, at this level of approximation, the quantum system possesses this type of order.

As an example, let us consider again the $J_1 - J_2$ model on the square lattice for $J_2/J_1 > 1/2$. The ground state is infinitely degenerate, the energy being independent of the angle θ between the two Néel sublattices (see left panel of Fig. 3). Although there are 4 sites per unit cell, thus in principle 4 branches of excitations, the Hamiltonian describing harmonic fluctuations has the periodicity of the square lattice, and the spectrum is simply given by $\omega_{\vec{k}} = \sqrt{B_{\vec{k}}^2 - A_{\vec{k}}^2}$ with

$$A_{\vec{k}}/S = -2J_1(\cos^2 \frac{\theta}{2} \cos k_x + \sin^2 \frac{\theta}{2} \cos k_y) - 4J_2 \cos k_x \cos k_y$$

and

$$B_{\vec{k}}/S = 2J_1(\sin^2 \frac{\theta}{2} \cos k_x + \cos^2 \frac{\theta}{2} \cos k_y) + 4J_2$$

The zero-point energy is minimal for $\theta = 0$ and $\theta = \pi$, which corresponds to the two helical ground states of wave vector $(0, \pi)$ and $(\pi, 0)$. Remarkably, these are the collinear states of the ground state manifold. This is a general trend. Whenever possible, coplanar states are favoured over non-coplanar ones and collinear states over non-collinear ones because their spectrum is softer, and their zero point energy lower [24].

The presence of two ground states and not simply one has an interesting consequence: these states can be distinguished by an Ising order parameter defined on the dual lattice,

$$\sigma_x = (\vec{S}_i - \vec{S}_j) \cdot (\vec{S}_j - \vec{S}_l) / |(\vec{S}_i - \vec{S}_j) \cdot (\vec{S}_j - \vec{S}_l)| \quad (10)$$

where (i, j, k, l) are the corners with diagonal (i, k) and (j, l) of the plaquette centered at the site x of the dual lattice. As a consequence, there is an Ising transition at finite temperature, a remarkable effect for a system with continuous symmetry [25, 26].

This harmonic selection process does not always lead to long-range order however. For instance, for the kagome lattice, the coplanar ground states are favoured, in agreement with the general trend, but the zero-point energy is exactly the same for all coplanar ground states [27]. One would have to push the expansion to higher order in $1/S$ to select among these states.

4.2 Thermal fluctuations

For a purely classical model, thermal fluctuations have a similar effect. Deviations from a classical ground state can be parametrized by two local coordinates according to

$$\vec{S}_i = \left(x_i, y_i, \sqrt{1 - x_i^2 - y_i^2} \right) \quad (11)$$

in the local reference frame of the ground state ($x_i = y_i = 0$ in the ground state). Expanding the energy to second order in x_i and y_i leads to a quadratic form for the energy. This allows to calculate the partition function as a gaussian integral. Although the coefficients of the quadratic form are not equal to the coefficients $A_{\vec{k}}$ and $B_{\vec{k}}$ of the quantum case, they are related to them, and, the low temperature free energy can be expressed in terms of the frequencies of the quantum case as ($k_B = 1$):

$$F = F_0 - \frac{1}{2} N_h T \ln T + T \sum_{\vec{k}} \ln \omega_{\vec{k}} \quad (12)$$

where F_0 is independent of the ground state, and N_h is the number of harmonic modes, i.e. of non-zero frequencies. In general, the state that minimizes $\sum_{\vec{k}} \ln \omega_{\vec{k}}$ is selected [24]. This is often the same state as the one selected by quantum fluctuations, but this does not need to be the case since quantum fluctuations minimize another function of the frequencies, namely their sum $\sum_{\vec{k}} \omega_{\vec{k}}$. Besides, zero frequencies play a different role. For the quantum case, they just give a vanishing contribution to the zero point energy, but for the classical case, they lead to an integral which is not gaussian. If the next term in the expansion of the non-quadratic modes is quartic, which is generically the case, the low temperature free-energy takes the form

$$F = F_0 - \frac{1}{2} N_h T \ln T - \frac{1}{4} N_q T \ln T + \dots \quad (13)$$

where N_q is the number of quartic modes. The factor $\frac{1}{2}$ is replaced by $\frac{1}{4}$ if the mode is quartic. As a consequence, the state with the maximal number of zero modes will always be favoured by thermal fluctuations [27], whereas this is not necessarily the case for quantum fluctuations.

5 Alternatives to magnetic long-range order in Heisenberg models

The presence of classical degeneracy in the ground state of a frustrated Heisenberg model typically leads to the presence of additional zero frequency spin-wave modes on top of those that

can be expected on general grounds (at $\vec{q} = \vec{0}$ and at $\vec{q} = \pm\vec{Q}$ in a helical state with pitch vector \vec{Q}). This degeneracy often leads to lines of zero modes (e.g. $J_1 - J_2$ model at $J_2 = J_1/2$) or even to a plane of zero modes (e.g. kagome) in the Brillouin zone, which, to harmonic order, implies a divergence of the correction to the local magnetization

$$\delta_m \equiv S - \langle S_i^z \rangle = \frac{1}{N} \sum_{\vec{k}} \langle a_{\vec{k}}^\dagger a_{\vec{k}} \rangle \quad (14)$$

since, in the ground state (the vacuum of the Bogoliubov α particles), $\langle a_{\vec{k}}^\dagger a_{\vec{k}} \rangle = v_{\vec{k}}^2 \propto 1/\omega_{\vec{k}}$. The spin-1/2 $J_1 - J_2$ model is believed to be disordered around $J_2 = J_1/2$ for that reason [28]. If the system is to maintain long-range order, higher-order corrections will have to open a gap at these accidental zero modes to restore a finite value of the corrections. Self-consistent calculations have been done that confirm this scenario, but for the calculation to be fully consistent, the corrections must still be smaller than the spin S , which is often not the case, at least for small enough spin. This implies that one has to look for alternatives to magnetic long-range order. One possibility is to break the SU(2) symmetry with an order parameter which is not the local spin, in which case one speaks of a spin nematic (see below). When the SU(2) symmetry is not broken, the resulting ground state is generically called a *spin liquid* [29]. The rest of this chapter reviews some of these possibilities.

5.1 Spin gap

A simple alternative to magnetic long-range order consists in opening a spin gap by adopting a ground state configuration in which spins are paired up to make local singlets rather than developing long-range order. In that respect, there is an important difference between systems with a half-integer or an integer spin per unit cell:

- If the total spin per unit cell is integer, then singlet pairing can be achieved without any spatial symmetry breaking, and the ground state is non degenerate. This is in particular the case of integer spin chains [30] and of spin ladders [31]. In spin ladders, there are two sites per unit cell, and the ground state is adiabatically connected to that of the strong rung limit, which simply consists of a product of singlets on the rungs. In integer spin chains, the simple picture relies on representing the local spin as a set of $2S$ spins 1/2, the ground state being adiabatically connected to the product of bond singlets constructed out of S spins 1/2 at each end of the bond [32]. In 2D, long-range antiferromagnetic order is generically realized in the absence of frustration (square lattice, honeycomb lattice), unless the system consists of weakly coupled dimers. With frustration however, the dimers do not need to be weakly coupled for this to be realized, as in the case of the Shastry-Sutherland model [33] (see below).
- If the total spin per unit cell is half-integer, singlet pairing can only be achieved through a spontaneous symmetry breaking that enlarges the unit cell to accommodate an integer total spin. The first and most famous example is the spin-1/2 $J_1 - J_2$ Heisenberg chain [34], which has in fact inspired the construction of the Shastry-Sutherland model.

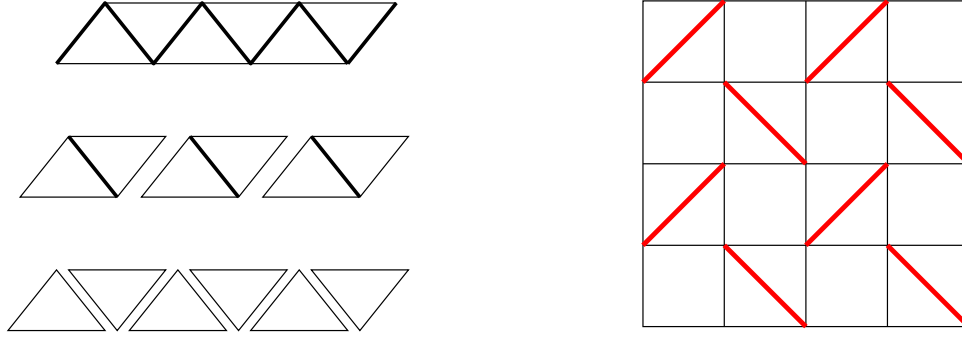


Fig. 5: Left panel: from top to bottom, sketch of the $J_1 - J_2$ chain, of its decomposition in terms of diamonds, and of its decomposition in terms of triangles. Thick solid lines stand for bonds of strength $J_1 = 2J_2$, thin solid lines for bonds of strength J_2 . Right panel: Shastry-Sutherland lattice.

The Majumdar-Ghosh model

The Hamiltonian of the spin-1/2 $J_1 - J_2$ Heisenberg chain is given by:

$$\mathcal{H}_{J_1-J_2} = \sum_i (J_1 \vec{S}_i \cdot \vec{S}_{i+1} + J_2 \vec{S}_i \cdot \vec{S}_{i+2}) \quad (15)$$

At the Majumdar-Ghosh point $J_2 = J_1/2$, the Hamiltonian can be rewritten (see middle left panel of Fig. 5)

$$\mathcal{H}_{J_1-J_2} = \sum_{i \text{ odd}} (J_1 \vec{S}_i \cdot \vec{S}_{i+1} + \frac{J_1}{2} (\vec{S}_i + \vec{S}_{i+1}) \cdot \vec{S}_{i-1} + \frac{J_1}{2} (\vec{S}_i + \vec{S}_{i+1}) \cdot \vec{S}_{i+2})$$

With this rewriting, it is clear that the wave function

$$|\psi_{\text{odd}}\rangle = \prod_{i \text{ odd}} |S(i, i+1)\rangle, \quad |S(i, i+1)\rangle = \text{singlet}$$

is an eigenstate of $\mathcal{H}_{J_1-J_2}$ of energy $E_{\text{odd}} = -(N/2)(3/4)J_1$, where N is the number of sites, since

$$(S_i^\alpha + S_{i+1}^\alpha) |S(i, i+1)\rangle = 0, \quad \alpha = x, y, z.$$

Now, the Hamiltonian can also be rewritten (see bottom left panel of Fig. 5)

$$\mathcal{H}_{J_1-J_2} = \sum_i \frac{J_1}{2} (\vec{S}_i \cdot \vec{S}_{i+1} + \vec{S}_i \cdot \vec{S}_{i+2} + \vec{S}_{i+1} \cdot \vec{S}_{i+2}) = \sum_i \mathcal{H}_\Delta(i).$$

Since the ground-state energy of a triangle of coupling $\frac{J_1}{2}$ is given by

$$E_0(\mathcal{H}_\Delta(i)) = -\frac{3}{4} \frac{J_1}{2}$$

the ground state energy of $\mathcal{H}_{J_1-J_2}$ satisfies the inequality

$$E_0(\mathcal{H}_{J_1-J_2}) \geq \sum_i E_0(\mathcal{H}_\Delta(i)) = -\frac{3}{4} \frac{J_1}{2} N = E_{\text{odd}}$$

which, by the variational principle, proves that $|\psi_{\text{odd}}\rangle$ is a ground state. The same reasoning can be done for

$$|\psi_{\text{even}}\rangle = \prod_{i \text{ even}} |S(i, i+1)\rangle$$

so that the ground state is two-fold degenerate.

More recently, this calculation has been generalized to arbitrary spin [35]. The trick is to consider the following generalization of the Hamiltonian

$$\mathcal{H}_{J_1-J_3} = J_1 \sum_i \vec{S}_i \cdot \vec{S}_{i+1} + J_3 \sum_i \left[(\vec{S}_{i-1} \cdot \vec{S}_i)(\vec{S}_i \cdot \vec{S}_{i+1}) + \text{h.c.} \right] \quad (16)$$

This Hamiltonian reduces to the $J_1 - J_2$ model with $J_2 = J_3/2$ for spin 1/2, but not for larger spin. It has been shown that the fully dimerized states are degenerate ground states for $J_3/J_1 = 1/(4S(S+1) - 2)$.

The Shastry-Sutherland model

In an attempt to find higher dimensional analogs of the Majumdar-Ghosh chain, Shastry and Sutherland came across a very interesting 2D model known as the Shastry-Sutherland model [33] and depicted in the right panel of Fig. 5. This model can be seen as an orthogonal dimer model, or as a square lattice with some diagonal couplings. Its Hamiltonian can be written as:

$$\mathcal{H}_{\text{Shastry-Sutherland}} = \sum_{\langle\langle i,j \rangle\rangle} J \vec{S}_i \cdot \vec{S}_j + \sum_{\langle i,j \rangle} J' \vec{S}_i \cdot \vec{S}_j \quad (17)$$

where $\langle\langle i,j \rangle\rangle$ stands for the diagonal bonds, and $\langle i,j \rangle$ for the bonds of the square lattice. The same type of argument as the first step of the proof of the Majumdar-Ghosh model shows that the product of singlets on J bonds is always an eigenstate, and variational arguments show that this will be the case as long as J'/J is not too large, less than 0.675 for spin-1/2 according to the most recent numerical estimate [36]. Remarkably enough, this model provides a very accurate description of the layered Cu oxide $\text{SrCu}_2(\text{BO}_3)_2$, a system in which the frustration not only opens a gap, but is also at the origin of a sequence of magnetization plateaux at 1/8, 2/15, 1/6, 1/4, 1/3, and 1/2 [37, 38].

5.2 Resonating Valence Bond spin liquids

For a spin-1/2 antiferromagnet with an odd number of spins per unit cell, as for instance the square and triangular lattices (1 spin per unit cell) and the kagome lattice (3 spins per unit cell), a product of singlet dimers has to break the spatial symmetry. In 1973, Anderson suggested that the spatial symmetry might be restored if the ground state is a superposition of all possible singlet dimer coverings that he called a Resonating Valence Bond (RVB) state (see Fig. 6), and he suggested that this might take place for the triangular lattice [39, 40]. It is now widely believed that the spin-1/2 Heisenberg model on the triangular lattice has 3-sublattice long-range order [41], but the RVB state remains a strong candidate for the spin-1/2 kagome antiferromagnet.

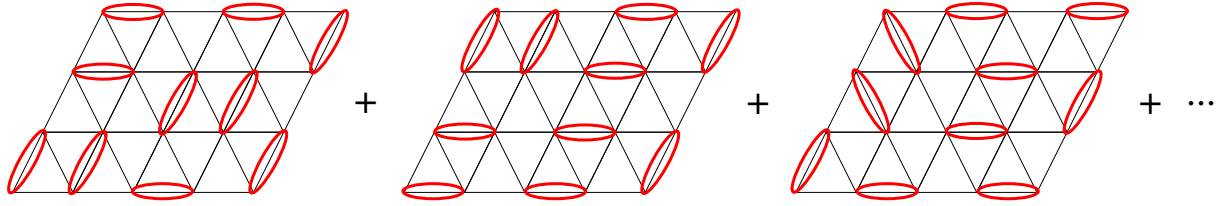


Fig. 6: Sketch of the Resonating Valence Bond (RVB) state on the triangular lattice. Red ellipses stand for singlet dimers for the Heisenberg model, and simply for dimers for the ground state of the Quantum Dimer Model on the triangular lattice at the Rokhsar-Kivelson point.

To prove directly that an RVB state is realized for a given spin-1/2 model is very challenging because it requires to perform numerical simulations on very large clusters, and Quantum Monte Carlo simulations cannot be performed for frustrated magnets because of the minus sign problem. However, the possibility to realize an RVB state has been demonstrated in effective models of the singlet sector known as Quantum Dimer Models (QDM). Let us thus start with a brief review of their properties.

The Hilbert space of a QDM is defined by all nearest-neighbor dimer coverings of a lattice, assumed to be orthogonal (note that this would not be the case for spin-1/2 singlets). The Hamiltonian typically contains kinetic terms that flip dimers around plaquettes, and potential terms proportional to the number of flippable plaquettes. The simplest model on a square lattice can be written as:

$$H_{\text{QDM}} = \sum_{\text{Plaquettes}} [-J (|\begin{smallmatrix} \vdots & \vdots \end{smallmatrix}\rangle \langle \begin{smallmatrix} \vdots & \vdots \end{smallmatrix}| + h.c.) + v (|\begin{smallmatrix} \vdots & \vdots \end{smallmatrix}\rangle \langle \begin{smallmatrix} \vdots & \vdots \end{smallmatrix}| + |\begin{smallmatrix} \vdots & \vdots \end{smallmatrix}\rangle \langle \begin{smallmatrix} \vdots & \vdots \end{smallmatrix}|)] \quad (18)$$

Rokhsar and Kivelson [42] asked the question whether, for some values of v/J , such a model can sustain a resonating valence bond (RVB) phase. As a first step toward an answer to this question, they proved the following theorem:

Theorem: For $v = J$ (RK-point), the sum of all configurations with equal weight is a ground state.

Proof: Consider $|\psi\rangle_{\text{RK}} = \sum_c |c\rangle$, where $|c\rangle$ is a dimer configuration. Let us write $H_{\text{QDM}} = \sum_i H_{\text{QDM}}^i$, where the sum over i runs over plaquettes, and consider a plaquette i . Then one can distinguish two types of configurations:

- c does not contain parallel dimers on plaquette i (plaquette i is not flippable in c). Then $H_{\text{QDM}}^i |c\rangle = 0$.
- c does contain parallel dimers. Then there is a companion configuration c' obtained from c by changing the orientation of dimers on plaquette i such that

$$\begin{aligned} H_{\text{QDM}}^i |c\rangle &= -J |c'\rangle + v |c\rangle \\ H_{\text{QDM}}^i |c'\rangle &= -J |c\rangle + v |c'\rangle \\ \Rightarrow H_{\text{QDM}}^i (|c\rangle + |c'\rangle) &= (v - J) (|c'\rangle + |c\rangle) \end{aligned}$$

Then, if $v = J$, $H_{\text{QDM}}^i(|c\rangle + |c'\rangle) = 0$. This implies that

$$H_{\text{QDM}}^i \sum_c |c\rangle = 0, \quad \forall i$$

and finally that

$$H_{\text{QDM}} |\psi\rangle_{\text{RK}} = 0.$$

So $|\psi\rangle_{\text{RK}}$ is an eigenstate with eigenvalue 0.

Let us now prove that this is the ground state energy. For that purpose, let us enlarge the Hilbert space to allow for empty sites (sites without dimers). Let us define the operator $a_{\uparrow\downarrow}$ as the operator that destroys $\uparrow\downarrow$ on a given plaquette provided there are such dimers on a given configuration, and that gives 0 otherwise, and let us denote the adjoint operator by $a_{\uparrow\downarrow}^\dagger$. Then the Hamiltonian

$$H = -J \sum_{\text{Plaquettes}} \left(a_{\uparrow\downarrow}^\dagger a_{\uparrow\downarrow} + a_{\uparrow\downarrow}^\dagger a_{\uparrow\downarrow} \right) + v \sum_{\text{Plaquettes}} \left(a_{\uparrow\downarrow}^\dagger a_{\uparrow\downarrow} + a_{\uparrow\downarrow}^\dagger a_{\uparrow\downarrow} \right)$$

is equal to H_{QDM} when restricted to the subspace where all sites belong to a dimer. So, the ground state energy of H_{QDM} must be larger or equal to the ground state of H . Now, for $v = J$, one can write

$$H = v \sum_{\text{Plaquettes}} \left(a_{\uparrow\downarrow}^\dagger - a_{\uparrow\downarrow}^\dagger \right) \left(a_{\uparrow\downarrow} - a_{\uparrow\downarrow} \right) = \sum_i A_i^\dagger A_i$$

with $A_i = a_{\uparrow\downarrow} - a_{\uparrow\downarrow}$, and the sum over i runs over all the plaquettes. Then,

$$\langle \psi | H | \psi \rangle = v \sum_i \langle \psi | A_i^\dagger A_i | \psi \rangle = v \sum_i \|A_i \psi\|^2 \geq 0$$

This implies that the ground state energy of H is positive, hence that the ground state energy of H_{QDM} is positive. Since the sum of all dimer configurations is a zero energy eigenstate, it is thus a ground state of H_{QDM} .

Does this imply that the QDM on the square lattice at the RK point is an RVB liquid? Not quite for several reasons. First of all, there are other ground states. Indeed all configurations with no flippable plaquette are zero energy eigenstates, and there are many of them. This is not a final blow however because their energy depends on the value of v/J in different ways. For $v > J$, these non-flippable configurations remain zero energy eigenstates and can be expected to be the only ground states, whereas for $v < J$, the state emanating from $|\psi\rangle_{\text{RK}}$ can be expected to be lower in energy than the non-flippable states.

More importantly, this RVB state can only be expected to extend into an RVB phase for $v < J$ if the spectrum is gapped at the RK point, *i.e.* if correlations decay exponentially. Now, the dimer-dimer correlations at the RK ground state are exactly the same as the classical dimer-dimer correlations averaged over all dimer coverings considered in Section 3. The decay is itself

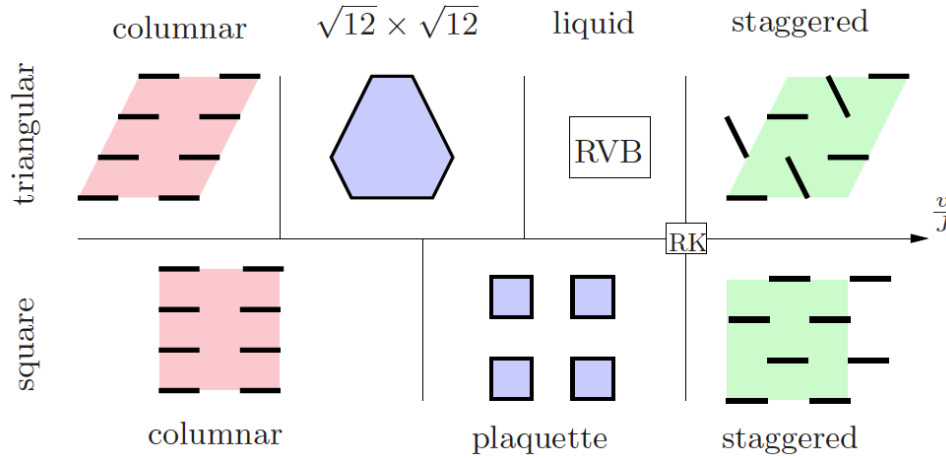


Fig. 7: Sketch of the phase diagram of the Rokhsar-Kivelson model on the triangular lattice (top) and on the square lattice (bottom). The staggered phases are degenerate, the configurations shown being the most symmetric ones.

related to the property of the Kasteleyn matrix: if all eigenvalues stay at a finite distance from 0, dimer-dimer correlations decay exponentially. Otherwise, they decay algebraically [43, 44]. For the square lattice, it is easy to show that, as for the honeycomb lattice, the spectrum of the Kasteleyn matrix has no gap. As a consequence, the correlations decay algebraically, the spectrum of H_{QDM} has no gap, and there is no RVB phase, a result confirmed by numerical simulations. By contrast, for the triangular lattice, the Kasteleyn matrix is gapped, and the correlations decay exponentially. The spectrum is thus gapped, and one can expect to stabilize an RVB phase below for $\nu < J$, in agreement with numerical results [45, 46] (see Fig. 7).

This state, although it is gapped, differs from a simple gapped state described e.g. by a product of singlet dimers by non-trivial topological properties:

- The ground state has a degeneracy that depends on the topology of the lattice (non degenerate on a finite lattice with open boundary conditions, two-fold degenerate on a cylinder, four-fold degenerate on a torus,...).
- The elementary excitations are fractionalized. On a finite system, they can only be created by pairs and consist in multiplying the configurations in the sum by $(-1)^{n_c}$, where n_c is the number of dimers cut along a line going from i to j , where i and j refer to the location of the elementary excitations called 'visons' [47].

Apart from spin models specifically constructed to have this property, the main candidate for an RVB spin liquid in quantum antiferromagnets is the spin-1/2 Heisenberg model on the kagome lattice, with strong numerical evidence from Density Matrix Renormalization Group calculations of a gap in both the singlet and triplet sectors [48]. The possibility to describe the singlet sector of this RVB liquid with the help of a Quantum Dimer Model is still debated. According to the first attempt at deriving an effective QDM, the system should be in a crystalline phase that breaks translational symmetry [49]. However, the derivation of an effective QDM has been

recently revisited, with the opposite conclusion that this effective model has indeed an RVB ground state [50].

5.3 Algebraic spin liquids

For half-integer spin, spin chains are not gapped, and spin-spin correlations decay to zero algebraically, by contrast to integer spin chains, in which they decay exponentially. It is thus natural to consider the possibility of algebraic decay as well in 2D frustrated magnets. To implement this goal, the most convenient way is to use a fermionic representation of spin-1/2 operators sometimes known as Abrikosov fermions:

$$\begin{cases} S_i^+ = c_{i\uparrow}^\dagger c_{i\downarrow} \\ S_i^- = c_{i\downarrow}^\dagger c_{i\uparrow} \\ S_i^z = \frac{1}{2} (n_{i\uparrow} - n_{i\downarrow}) \end{cases} \quad (19)$$

with the constraint $n_{i\uparrow} + n_{i\downarrow} = 1$. In this representation, the Heisenberg model takes the form:

$$H = \frac{1}{2} \sum_{i,j} J_{ij} \left[\frac{1}{2} (c_{i\uparrow}^\dagger c_{i\downarrow} c_{j\downarrow}^\dagger c_{j\uparrow} + \text{h.c.}) + \frac{1}{4} (c_{i\uparrow}^\dagger c_{i\uparrow} - c_{i\downarrow}^\dagger c_{i\downarrow}) (c_{j\uparrow}^\dagger c_{j\uparrow} - c_{j\downarrow}^\dagger c_{j\downarrow}) \right] \quad (20)$$

This Hamiltonian is not quadratic, and the only simple (but of course approximate) solution relies on performing a mean-field decoupling of the four-fermion operators, and on treating the constraint on average with a Lagrange parameter. To describe algebraic liquids, it is convenient to introduce the bond operator

$$\chi_{ij} = c_{i\uparrow}^\dagger c_{j\uparrow} + c_{i\downarrow}^\dagger c_{j\downarrow} \quad (21)$$

which satisfies the identity:

$$\vec{S}_i \cdot \vec{S}_j = \frac{1}{4} - \frac{1}{2} \chi_{ij}^\dagger \chi_{ij} \quad (22)$$

and to decouple the Hamiltonian by introducing the order parameter $\chi_{ij}^0 = \langle \chi_{ij} \rangle$.

Following Affleck and Marston in their seminal work [51], let us consider the square lattice. As is often the case with mean-field theory, the self-consistent equations possess several solutions. Let us concentrate on two of them:

- $\chi_{ij}^0 = \chi_0$ on a set of bonds that constitute a dimer covering of the lattice, and $\chi_{ij}^0 = 0$ on the other bonds. This solution describes a spontaneously dimerized state.
- $\chi_{ij}^0 = \chi_0 e^{i\theta_{ij}}$, where the phases θ_{ij} are chosen in such a way that they lead to a π -flux per plaquette. A possible choice of gauge is given by $\theta_{ij} = \pi/4$ if the arrow goes from i to j in Fig. 8 (left panel). This solution is called the π flux state. The dispersion of the fermionic spectrum is given by:

$$E = \pm J \chi_0 \sqrt{\cos^2 k_x + \cos^2 k_y} \quad (23)$$

This spectrum is a Dirac spectrum, with 4 Dirac points. Since the system must be half-filled to satisfy the constraint $n_{i\uparrow} + n_{i\downarrow} = 1$, the Fermi energy is given by $E_F = 0$, and the Fermi surface consists of 4 points, $k_x, k_y = \pm\pi/2$.

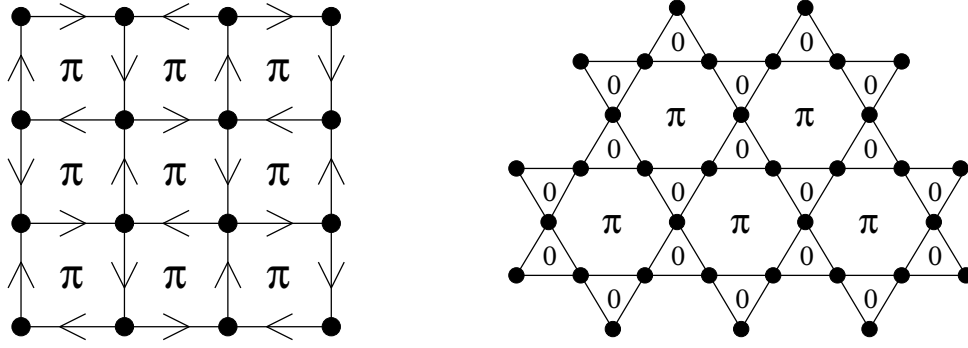


Fig. 8: *Left panel: Affleck-Marston π -flux phase on the square lattice. The phase of the hopping integral is equal to $\pi/4$ on each bond in the direction of the arrow. Right panel: flux pattern of the algebraic spin liquid proposed as a ground state for the spin-1/2 Heisenberg model on the kagome lattice.*

In this mean-field ground state, the spin-spin correlations decay algebraically, which gives rise to power laws at low temperature. It has been argued that, because of the Dirac nature of the spectrum, this mean-field solution is locally stable [53], and that the state described by this solution could be considered as a consistent theory of an algebraic spin liquid. Note that the order parameter χ_{ij} is invariant under the gauge transformation $c_{i\uparrow}^\dagger \rightarrow e^{i\theta} c_{i\uparrow}^\dagger$, where θ can take any value. There is thus a $U(1)$ gauge symmetry in the problem, and this type of spin liquid is sometimes referred to as a $U(1)$ spin liquid. The order parameter breaks however the original $SU(2)$ symmetry, and different order parameters can correspond to the same physical solutions. A proper classification of the solutions relies on the projective symmetry group introduced by Wen [52].

To compare the various solutions, one can of course compare the mean-field energies. However, these energies are not variational because the local constraint is only satisfied on average, and the wave functions obtained within mean-field contain a lot of configurations with doubly occupied sites. A numerically tractable way to go beyond the mean-field approximation consists into projecting into the sector with no doubly occupied sites using the Gutzwiller projector:

$$P_G = \prod_i (1 - n_{i\uparrow} n_{i\downarrow}) \quad (24)$$

The energy of the state $P_G|\psi_{\text{MF}}\rangle$, where $|\psi_{\text{MF}}\rangle$ is a mean-field solution, can be evaluated with a Monte Carlo simulation [54]. In fact, one can generalize the method and use as a variational subspace a set of functions of the form $P_G|\psi_{\text{fermion}}\rangle$, where $|\psi_{\text{fermion}}\rangle$ is the ground state of quadratic fermionic hamiltonians not necessarily related to a mean-field solution of the original problem. This method goes under the name of Variational Monte Carlo (VMC) [55].

For the square lattice, the best VMC state is a flux-state with a uniform flux less than π per plaquette. This is clearly not the true ground state, which has long-range Néel order. However, the VMC approach, as a way to look for alternatives to long-range magnetic order, is very versatile since it allows to compare several types of quantum liquids (including the RVB states discussed in the previous section and the chiral states discussed in the next one). It has been implemented

for the spin-1/2 kagome antiferromagnet, with the conclusion that the lowest energy state is the one depicted in the right panel of Fig. 8, with a flux π per hexagon and no flux through the triangles [56]. The resulting state is an algebraic spin liquid, and it is one of the main candidates for the ground state of the spin-1/2 kagome antiferromagnet.

Note that one can also introduce a pairing operator $\eta_{ij} = c_{i\uparrow}^\dagger c_{j\downarrow}^\dagger - c_{i\downarrow}^\dagger c_{j\uparrow}^\dagger$ to decouple the Hamiltonian. This leads to a mean-field theory of the RVB state discussed in the previous section. This order parameter is only invariant upon the transformation $c_{i\uparrow}^\dagger \rightarrow e^{i\theta} c_{i\uparrow}^\dagger$ with $\theta = \pi$, i.e. $c_{i\uparrow}^\dagger \rightarrow -c_{i\uparrow}^\dagger$. There is thus only a Z_2 gauge symmetry, and these states are sometimes referred to as Z_2 spin liquids.

5.4 Chiral spin liquids

All the states discussed so far as alternatives to magnetic long-range leave the time-reversal symmetry unbroken. It has been suggested however that another family of quantum spin liquids related to Fractional Quantum Hall (FQH) states might be stabilized by frustration [57]. These states break time-reversal and parity, but not their product. A possible order parameter is the mixed product $\vec{S}_1 \cdot (\vec{S}_2 \times \vec{S}_3)$, also called the scalar chirality [58].

Although the symmetry-based definition is the most fundamental one, the discussion of the properties of chiral spin liquids is most conveniently done using the language of Gutzwiller projected wave-functions. In that language, a chiral state is obtained by applying a Gutzwiller projection to a fermionic state that is the ground state of a Hamiltonian with a fractional flux through some plaquettes, i.e. a flux which is neither equal to 0 nor to π , so that time reversal symmetry is broken [59]. In the mean-field language, the order parameter is of the χ_{ij} type, but it has to break translational symmetry to accommodate a fractional flux per plaquette. The resulting band structure is gapped, and the effective low-energy theory is a pure gauge theory. As a consequence, the ground state is expected to have a topological degeneracy equal to twice that of the corresponding FQH state, the extra factor 2 coming from the broken time-reversal symmetry. The elementary excitations are anyons, with fractional statistics.

The best evidences so far in favour of such ground states in frustrated magnets have been obtained for extensions of the Heisenberg model on the kagome lattice, possibly a consequence of the fact that, when further neighbor couplings are introduced, the classical kagome antiferromagnet has non coplanar ground states [60]. In particular, when second and third neighbor interactions are present, and for specific values of the couplings, the best VMC state is a flux state with a complicated flux pattern. This chiral state has been confirmed by numerical results, which have reported a set of four lying states, in agreement with the expected 4-fold degenerate ground state in the thermodynamic limit [61].

Another model consists of a generalization of the Heisenberg model that explicitly breaks the chiral symmetry by introducing a term of the form $\vec{S}_i \cdot (\vec{S}_j \times \vec{S}_k)$ on each plaquette. Since the chiral symmetry is explicitly broken, one expects the ground state to be only two-fold degenerate, in agreement with DMRG results [62].

Note that the situation is quite different in 3D, where the gauge theory is equivalent to electro-

magnetism, and where one can expect to have a linearly dispersive mode sometimes referred to as 'photon' [63].

5.5 Nematic order

Another, completely different possibility for a system to avoid magnetic ordering is to break the SU(2) symmetry without developing long-range magnetic order. This simply requires that the operator that develops long-range correlations is not simply the local spin operator, but a more complicated local operator, very much like liquid crystals, which break spatial symmetries but do not have standard crystalline order. By order of increasing complexity, the next possibility is an operator constructed out of two spin operators [64]. Let us thus consider 2 spins \vec{S}_i and \vec{S}_j . By combining them, one can construct *a priori* 9 operators:

$$S_i^\alpha S_j^\beta, \quad \alpha, \beta = x, y, z \quad (25)$$

Out of these 9 operators, one can construct a scalar, a vector, and a rank 2 tensor:

- $\vec{S}_i \cdot \vec{S}_j$: This is a scalar, and it cannot break the SU(2) symmetry.
- $\vec{S}_i \times \vec{S}_j$: This operator has three components and is a vector. If such an operator develops long-range correlations, the system is said to be *p-nematic*.
- The last five independent operators constitute a rank-2 tensor. They can be conveniently arranged in a five-component vector:

$$\vec{Q}_{ij} = \begin{pmatrix} S_i^x S_j^x - S_i^y S_j^y \\ \frac{1}{\sqrt{3}} (3S_i^z S_j^z - \vec{S}_i \cdot \vec{S}_j) \\ S_i^x S_j^y + S_i^y S_j^x \\ S_i^y S_j^z + S_i^z S_j^y \\ S_i^z S_j^x + S_i^x S_j^z \end{pmatrix} \quad (26)$$

If this operator develops long-range order, the system is said to be *n-nematic*

Now, let us briefly see which possibilities can be realized depending on the value of the spin, and on whether the sites i and j are equal or different.

- *Classical spin systems*: A purely local order parameter of the p-nematic type cannot be realized because $\vec{S}_i \times \vec{S}_i = \vec{0}$. However, a purely local n-nematic order parameter $\vec{Q}_i \equiv \vec{Q}_{ii}$, whose components involve products of components of the spin at site i , can be realized. If we relax the requirement of a purely local order parameter, then both the vector chirality $\vec{S}_i \times \vec{S}_j$ and the quadrupolar operator \vec{Q}_{ij} can be realized.
- *S=1/2 systems*: For spins 1/2, there are no new purely local order parameters: $\vec{S}_i \times \vec{S}_i = i\hbar\vec{S}_i$ is proportional to the local spin, and \vec{Q}_i vanishes identically because $(S_i^\alpha)^2 = 1/4$ and $S_i^\alpha S_i^\beta = -S_i^\beta S_i^\alpha$ for spin-1/2 operators. So the only possible nematic operators are bond operators, the vector chirality $\vec{S}_i \times \vec{S}_j$ and the bond quadrupolar operator \vec{Q}_{ij} .

- $S=1$ systems: The identity $\vec{S}_i \times \vec{S}_i = i\hbar\vec{S}_i$ still holds, so there is no p-nematic local order parameter, but, by contrast to the spin-1/2 case, the local quadrupolar operator \vec{Q}_i does not vanish identically. For $i \neq j$, as for spin 1/2, both the bond vector chirality and the bond quadrupolar operators can be realized.
- $S>1$ systems: There is no difference with the spin-1 case regarding operators that involve two spins. There is a difference however when one considers more than 2 spins. For spin $S > 1$, purely local operators involving $2S > 2$ spins can be constructed, corresponding to octupolar order, etc.

Two cases have been discussed at length in the recent literature: purely local quadrupolar order in spin-1 antiferromagnets, and bond n-nematic order in spin-1/2 antiferromagnets.

Local quadrupolar order parameter in spin-1 bilinear-biquadratic models

The possibility for a spin-1 system to develop purely quadrupolar order can be understood in very simple terms. Indeed, let us consider the S^z basis $\{|-1\rangle, |0\rangle, |1\rangle\}$ of a spin 1. The states $|-1\rangle$ and $|1\rangle$ are clearly magnetic and correspond to a spin pointing opposite to z or along z . By contrast, the state $|0\rangle$ is not magnetic. Indeed, one can easily check that it satisfies $\langle 0|S^\alpha|0\rangle = 0$ for $\alpha = x, y, z$. However, it is not invariant by rotation. Indeed, $\langle 0|(S^x)^2|0\rangle = \langle 0|(S^y)^2|0\rangle = 1$, while $\langle 0|(S^z)^2|0\rangle = 0$. This state is a quantum state that describes fluctuations perpendicular to z . Note that there is no sign attached to the direction perpendicular to which fluctuations take place, and this direction is called the *director* of the quadrupolar state. This director can point in any direction, and one can in fact define a purely quadrupolar, time-reversal invariant basis with directors along x, y and z :

$$|x\rangle = i\frac{|1\rangle - |\bar{1}\rangle}{\sqrt{2}}, \quad |y\rangle = \frac{|1\rangle + |\bar{1}\rangle}{\sqrt{2}}, \quad |z\rangle = -i|0\rangle \quad (27)$$

In this basis, a general state can be decomposed as

$$|\vec{d}\rangle = d_x|x\rangle + d_y|y\rangle + d_z|z\rangle$$

where \vec{d} is a complex vector of norm 1. To keep track of the nature of the state (magnetic, quadrupolar, or mixed), it is convenient to parametrize \vec{d} according to [65]:

$$\vec{d} = \vec{u} + i\vec{v}, \quad \vec{u} \text{ and } \vec{v} \text{ real}, \quad \|\vec{u}\|^2 + \|\vec{v}\|^2 = 1, \quad \vec{u} \cdot \vec{v} = 0$$

Then, $\langle \vec{d}|\vec{S}|\vec{d}\rangle = 2\vec{u} \times \vec{v}$. A state is purely magnetic if $\|\vec{u}\|^2 = \|\vec{v}\|^2 = \frac{1}{2}$, and it is purely quadrupolar if $\vec{u} = \vec{0}$ or $\vec{v} = \vec{0}$, with director along the non-zero vector.

Let us now consider the bilinear-biquadratic spin-1 model on the triangular lattice defined by the Hamiltonian:

$$H = \sum_{\langle i,j \rangle} [J_{\text{bil}}\vec{S}_i \cdot \vec{S}_j + J_{\text{biq}}(\vec{S}_i \cdot \vec{S}_j)^2] \quad (28)$$

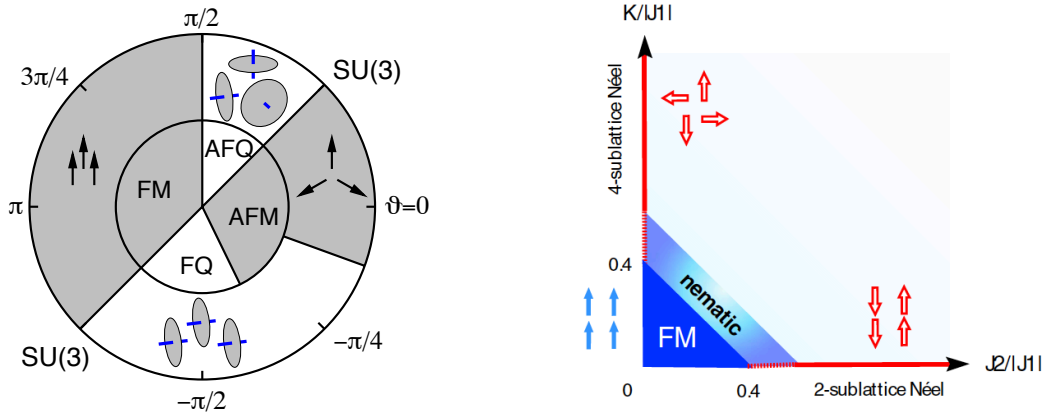


Fig. 9: Left panel: phase diagram of the bilinear-biquadratic spin-1 Heisenberg model on the triangular lattice. The angle θ keeps track of the relative magnitude of the bilinear coupling ($J_{\text{bil}} \propto \cos \theta$) to the biquadratic one ($J_{\text{biq}} \propto \sin \theta$). The inner circle is the mean-field phase diagram, the outer one the numerical one obtained with flavour-wave theory and exact diagonalizations. There are two quadrupolar phases: a ferroquadrupolar phase for negative biquadratic coupling, and a 3-sublattice antiferroquadrupolar one for positive biquadratic coupling. (After Läuchli et al. [67]) Right panel: sketch of the phase diagram of the spin-1/2 Heisenberg model on the square lattice with ferromagnetic nearest-neighbor coupling $J_1 < 0$, antiferromagnetic next-nearest neighbor coupling J_2 , and four-spin plaquette interaction K . There is a nematic phase close to the ferromagnetic one. (After Shannon et al. [69])

The presence of quadrupolar order with a local order parameter is plausible if biquadratic interactions are present because the Hamiltonian can be rewritten with the help of quadrupolar operators using the identity

$$J_{\text{bil}} \vec{S}_1 \cdot \vec{S}_2 + J_{\text{biq}} (\vec{S}_1 \cdot \vec{S}_2)^2 = \left(J_{\text{bil}} - \frac{J_{\text{biq}}}{2} \right) \vec{S}_1 \cdot \vec{S}_2 + \frac{J_{\text{biq}}}{2} \vec{Q}_1 \cdot \vec{Q}_2 + \frac{4}{3} J_{\text{biq}} \quad (29)$$

Then, the first step is to determine a mean-field phase diagram by looking for the product state that minimizes the energy as function of θ , with $J_{\text{bil}} = J \cos \theta$ and $J_{\text{biq}} = J \sin \theta$. This minimization is easily done using the following expectation values:

$$\begin{aligned} \langle \vec{d}_1, \vec{d}_2 | \vec{S}_1 \cdot \vec{S}_2 | \vec{d}_1, \vec{d}_2 \rangle &= |\vec{d}_1 \cdot \vec{d}_2^*|^2 - |\vec{d}_1 \cdot \vec{d}_2|^2 = 4(\vec{u}_1 \times \vec{v}_1) \cdot (\vec{u}_2 \times \vec{v}_2) \\ \langle \vec{d}_1, \vec{d}_2 | (\vec{S}_1 \cdot \vec{S}_2)^2 | \vec{d}_1, \vec{d}_2 \rangle &= 1 + |\vec{d}_1 \cdot \vec{d}_2|^2 = 1 + (\vec{u}_1 \cdot \vec{u}_2 - \vec{v}_1 \cdot \vec{v}_2)^2 + (\vec{u}_1 \cdot \vec{v}_2 + \vec{v}_1 \cdot \vec{u}_2)^2 \end{aligned}$$

The conclusion is that, if J_{biq} is large and positive, directors tend to be perpendicular on neighboring sites, while if J_{biq} is large and negative, directors tend to be parallel. The resulting phase diagram on the triangular lattice is depicted in the left panel of Fig. 9. In addition to the standard ferromagnetic and 3-sublattice antiferromagnetic phase, it contains a ferroquadrupolar phase, and a 3-sublattice antiferroquadrupolar phase. These simple results have been confirmed by more sophisticated calculations [66, 67].

Bond nematic phases

For spin-1/2 antiferromagnets, there is no purely local order parameter. However, bond operators can give rise to nematic order. An instability towards a p-nematic has been suggested early on for the square and kagome lattices with further neighbor interactions in the context of a semi-classical analysis [68]. More recently, extensive numerical results for spin-1/2 have suggested that there is an instability towards an n-nematic phase for the $J_1 - J_2$ model on the square lattice for negative (ferromagnetic) J_1 and positive J_2 , close to the ferromagnetic phase [69]. The absence of a purely local order parameter prevents one from performing a simple analysis in terms of a product wave-function. In that case, it is the proximity of a ferromagnetic state that leads to a simple picture: the instability that is responsible for the disappearance of ferromagnetism is a condensation of two-magnon bound states, and the order parameter that describes the resulting order is a two-spin n-nematic operator (see right panel of Fig. 9). A similar effect has been predicted close to saturation.

6 Conclusion

It should be clear to the reader at that stage that frustrated magnetism has become a vast subject over the years, and although I have tried to cover (sometimes very briefly) several aspects of current interest, I am aware of the fact that entire subfields have been left aside. For instance, I have chosen to concentrate on the Ising and Heisenberg models, but frustration is also a source of fascinating phenomena for the XY model [70], with a number of specificities that I would not have been able to cover properly. For similar reasons, I have also decided to say very little about experimental results, but of course frustrated magnetism is to a large extent an experimental subject [71]. If, in spite of all its imperfections and shortcomings, this chapter manages to make some of the advanced theoretical concepts of frustrated magnetism accessible to non specialists, it will have reached its main objective.

It is a pleasure to thank all the colleagues with whom I have had the privilege to interact on frustrated magnetism over the years, in particular M. Albrecht, V. I. Anisimov, F. Becca, C. Berthier, P. Carretta, S. Capponi, J. Cisarova, T. Coletta, P. Corboz, S. Dommange, J. Dorier, M. Elhajal, P. Fazekas, M. Ferrero, J.-B. Fouet, J. Gavilano, A. Honecker, M. Horvatic, D. Ivanov, S. Korshunov, V. Kotov, B. Kumar, C. Lacroix, N. Laflorencie, A. Läuchli, C. Lhuillier, M. Mambrini, S. Manmana, V. Mazurenko, P. Mendels, L. Messio, F. Michaud, P. Millet, G. Misguich, S. Miyahara, R. M. Noack, B. Normand, H. R. Ott, K. Penc, J.-D. Picon, D. Poilblanc, A. Ralko, I. Rousochatzakis, K. Schmidt, J. Strecka, M. Takigawa, O. Tchernyshyov, T. Toth, M. Troyer, F. Vernay, C. Weber, S. Wenzel, H. Y. Yang, F. C. Zhang, and M. Zhitomirsky. This work has been supported by the Swiss National Science Foundation.

References

- [1] J.-F. Sadoc and R. Mosseri, Geometrical Frustration, (Cambridge University Press, 1999).
- [2] G. H. Wannier, Phys. Rev. **79**, 357 (1950).
- [3] R. Moessner, S. L. Sondhi, and P. Chandra, Phys. Rev. Lett. **84**, 4457 (2000).
- [4] M. E. Fisher, Phys. Rev. **124**, 1664 (1961).
- [5] P. W. Kasteleyn, J. Math. Phys. **4**, 287 (1963).
- [6] L. Pauling, J. Am. Chem. Soc. **57**, 2680 (1935).
- [7] J. S. Gardner, M. J. P. Gingras and J. E. Greedan, Rev. Mod. Phys. **82**, 53 (2010).
- [8] J. F. Nagle, Journal of Mathematical Physics **7**, 1484 (1966).
- [9] A. P. Ramirez, A. Hayashi, R. J. Cava, R. Siddharthan, and B. S. Shastry, Nature **399**, 333 (1999).
- [10] J. M. Luttinger and L. Tisza, Phys. Rev. **70**, 954 (1946).
- [11] R. J. Baxter, J. Math. Phys. **11**, 784 (1970).
- [12] A. Sütö, Z. Phys. B **44**, 121 (1981).
- [13] R. Kotecký, J. Salas, and A. D. Sokal, Phys. Rev. Lett. **101**, 030601 (2008).
- [14] S. Korshunov, F. Mila, and K. Penc, Phys. Rev. B **85**, 174420 (2002).
- [15] J. Stephenson, J. Math. Phys. **5**, 1009 (1964).
- [16] C. L. Henley, J. Stat. Phys. **89**, 483 (1997).
- [17] R. Moessner and S. L. Sondhi, Phys. Rev. B **63**, 224401 (2001).
- [18] H. W. J. Blöte and H. J. Hilhorst, J. Phys. A: Math. Gen. **15**, L631 (1982).
- [19] S.V. Isakov, K. Gregor, R. Moessner, and S. L. Sondhi, Phys. Rev. Lett. **93**, 167204 (2004).
- [20] D. A. Garanin and B. Canals, Phys. Rev. B **59**, 443 (1999).
- [21] T. Fennell, P. P. Deen, A. R. Wildes, K. Schmalzl, D. Prabhakaran, A. T. Boothroyd, R. J. Aldus, D. F. McMorrow, and S. T. Bramwell, Science **326**, 415 (2009).
- [22] E. F. Shender, Zh. Eksp. Teor. Fiz. **83**, 326 (1982) [Sov. Phys. JETP **56**, 178 (1982)].
- [23] J. Villain, R. Bidaux, J. P. Carton and R. Conte, J. Phys. (Paris) **41**, 1263 (1980).
- [24] C. L. Henley, Phys. Rev. Lett. **62**, 2056 (1989).

- [25] P. Chandra, P. Coleman, and A. I. Larkin, Phys. Rev. Lett. **64**, 88 (1990).
- [26] C. Weber, L. Capriotti, G. Misguich, F. Becca, M. Elhajal, and F. Mila, Phys. Rev. Lett. **91**, 177202 (2003).
- [27] J. T. Chalker, P. C. W. Holdsworth, and E. F. Shender, Phys. Rev. Lett. **68**, 855 (1992).
- [28] P. Chandra and B. Douçot, Phys. Rev. B **38**, 9335(R) (1988).
- [29] L. Balents, Nature **464**, 199 (2010).
- [30] F. D. M. Haldane., Phys. Lett. A **93**, 464 (1983).
- [31] E. Dagotto and T. M. Rice, Science **271**, 618 (1996).
- [32] I. Affleck, T. Kennedy, E. H. Lieb, and H. Tasaki, Phys. Rev. Lett. **59**, 799 (1987).
- [33] B. Sriram Shastry and B. Sutherland, Physica (Amsterdam) **108B+C**, 1069 (1981).
- [34] C. K. Majumdar and D. K. Ghosh, J. Math. Phys. (N.Y.) **10**, 1388 (1969).
- [35] F. Michaud, F. Vernay, S. R. Manmana, and F. Mila, Phys. Rev. Lett. **108**, 127202 (2012).
- [36] P. Corboz and F. Mila, Phys. Rev. B **87**, 115144 (2013).
- [37] H. Kageyama, K. Yoshimura, R. Stern, N. V. Mushnikov, K. Onizuka, M. Kato, K. Kosuge, C. P. Slichter, T. Goto, and Y. Ueda, Phys. Rev. Lett. **82**, 3168 (1999).
- [38] For a recent review, see M. Takigawa and F. Mila, Introduction to Frustrated Magnetism, edited by C. Lacroix, P. Mendels, and F. Mila, p. 241 (Springer, New York, 2011).
- [39] P. W. Anderson, Mater. Res. Bull. **8**, 153 (1973).
- [40] P. Fazekas and P. W. Anderson, Philos. Mag. **30**, 23 (1974).
- [41] B. Bernu, C. Lhuillier, and L. Pierre, Phys. Rev. Lett. **69**, 2590 (1992).
- [42] D. S. Rokhsar and S. A. Kivelson, Phys. Rev. Lett. **61**, 2376 (1988).
- [43] P. Fendley, R. Moessner, and S. L. Sondhi, Phys. Rev. B **66**, 214513 (2002).
- [44] A. Ioselevich, D. A. Ivanov, and M. V. Feigelman, Phys. Rev. B **66**, 174405 (2002).
- [45] R. Moessner and S. L. Sondhi, Phys. Rev. Lett. **86**, 1881 (2001).
- [46] A. Ralko, M. Ferrero, F. Becca, D. Ivanov, and F. Mila, Phys. Rev. B **71**, 224109 (2005).
- [47] T. Senthil and M. P. A. Fisher, Phys. Rev. B **62**, 7850 (2000).
- [48] S. Yan, D. A. Huse, and S. R. White, Science **332**, 1173 (2011).

- [49] D. Schwandt, M. Mambrini, and D. Poilblanc, *Phys. Rev. B* **81**, 214413 (2010).
- [50] I. Rousochatzakis, Y. Wan, O. Tchernyshyov, and F. Mila, *Phys. Rev. B* **90**, 100406(R) (2014).
- [51] J. B. Marston and I. Affleck, *Phys. Rev. B* **39**, 11538 (1989).
- [52] X.-G. Wen, *Phys. Rev. B* **44**, 2664 (1991).
- [53] M. Hermele, T. Senthil, and M. P. A. Fisher, *Phys. Rev. B* **72**, 104404 (2005).
- [54] C. Gros, *Ann. Phys. (N.Y.)* **189**, 53 (1989).
- [55] For a recent review, see F. Becca, L. Capriotti, A. Parola, and S. Sorella, *Introduction to Frustrated Magnetism*, edited by C. Lacroix, P. Mendels, and F. Mila, p. 379 (Springer, New York, 2011).
- [56] Y. Ran, M. Hermele, P. A. Lee, and X.-G. Wen, *Phys. Rev. Lett.* **98**, 117205 (2007).
- [57] V. Kalmeyer and R. B. Laughlin, *Phys. Rev. Lett.* **59**, 2095 (1987).
- [58] X. G. Wen, F. Wilczek, and A. Zee, *Phys. Rev. B* **39**, 11413 (1989).
- [59] X. G. Wen, *Phys. Rev. B* **40**, 7387 (1989).
- [60] L. Messio, C. Lhuillier, and G. Misguich, *Phys. Rev. B* **83**, 184401 (2011).
- [61] S.-S. Gong, W. Zhu, and D. N. Sheng, *Sci. Rep.* **4**, 6317 (2014).
- [62] B. Bauer, L. Cincio, B. P. Keller, M. Dolfi, G. Vidal, S. Trebst, and A. W. W. Ludwig, *Nature Communications* **5**, 5137 (2014).
- [63] M. Hermele, M.P.A. Fisher, and L. Balents, *Phys. Rev. B* **69**, 064404 (2004).
- [64] A.F. Andreev and I.A. Grishchuk, *Zh. Eksp. Teor. Fiz.* **87**, 467 (1984) [*Sov. Phys. JETP* **60**, 267 (1984)].
- [65] B. A. Ivanov and A.K. Kolezhuk, *Phys. Rev. B* **68**, 052401 (2003).
- [66] H. Tsunetsugu and M. Arikawa, *J. Phys. Soc. Jpn.* **75**, 083701 (2006).
- [67] A. Läuchli, F. Mila, and K. Penc, *Phys. Rev. Lett.* **97**, 087205 (2006).
- [68] P. Chandra and P. Coleman, *Phys. Rev. Lett.* **66**, 100 (1991).
- [69] N. Shannon, T. Momoi, and P. Sindzingre, *Phys. Rev. Lett.* **96**, 027213 (2006).
- [70] For a review, see S. Korshunov, *Physics - Uspekhi* **49** (3), 225 (2006).
- [71] For a recent review of all aspects of the fields (materials, experiments and theory), see *Introduction to Frustrated Magnetism*, edited by C. Lacroix, P. Mendels, and F. Mila, (Springer, New York, 2011).

Index

algebraic correlations, 8
algebraic spin liquid, 22

checkerboard lattice, 10
chiral spin liquid, 23
competing interactions, 3

degeneracy, 3
dimer covering, 3, 18
dipolar correlations, 11

frustration, 2

geometrical frustration, 2
Gutzwiller projection, 22, 23

height model, 8
Heisenberg model, 2, 6
helical, 6

Ising model, 3, 8, 10

 J_1 - J_2 model, 6, 13

kagome lattice, 7, 20
Kasteleyn matrix, 4, 8, 20

Majumdar-Ghosh point, 16

nematic, 24

order by disorder, 12

pyrochlore lattice, 5, 8, 11

quadrupolar, 25
quantum dimer model, 18
quantum fluctuations, 12

residual entropy, 5
resonating valence bond, 17

Shastry-Sutherland model, 17
spin gap, 15
spin ice, 5

thermal fluctuations, 14
triangular lattice, 3, 8

U(1) spin liquid, 22

 Z_2 spin liquid, 23